Available online at www.sciencedirect.com
ScienceDirect
Trans. Nonferrous Met. Soc. China 30(2020) 905−916
Transactions of Nonferrous Metals Society of China
www.tnmsc.cn

Effect of second-phase particle size and presence of vibration on AZ91/SiC surface composite layer produced by FSP

Behrouz BAGHERI[1], Mahmoud ABBASI[2], Amin ABDOLLAHZADEH[3,4], Seyyed Ehsan MIRSALEHI[1]

1. Department of Mining and Metallurgy, Amirkabir University of Technology, Tehran, Iran;
2. Faculty of Engineering, University of Kashan, Kashan, Iran;
3. Department of Materials Science and Engineering, Sharif University of Technology, Tehran, Iran;
4. Institute of Materials Engineering and Advanced Processes, Department of Mining and Metallurgy, Amirkabir University of Technology, Tehran, Iran

Received 23 August 2019; accepted 4 March 2020

Abstract: An improved method of friction stir processing (FSP) was introduced for the processing of AZ91 magnesium alloy specimens. This novel process was called "friction stir vibration processing (FSVP)". FSP and FSVP were utilized to develop surface composites on the studied alloy while SiC nanoparticles were applied as second-phase particles. The effect of reinforcing SiC particles with different sizes (30 and 300 nm) on different characteristics of the composite surface was studied. The results indicated that the microstructure was refined and mechanical properties such as hardness, ductility, and strength were enhanced as FSVP was applied. Furthermore, it was concluded that the effect of reinforcing particles with a size of 30 nm on the microstructure and mechanical properties of the surface composite was more obvious than that of particles with a size of 300 nm. It was also found that mechanical properties and microstructure of FSV-processed specimens were improved as vibration frequency increased. The hardness value in the stir zone was about 157 MPa for the FSV-processed specimen at a vibration frequency of 50 Hz, while this value was around 116 MPa for the FSV-processed specimen at a vibration frequency of 25 Hz.

Key words: friction stir processing; vibration; SiC nano-particles; particle size; mechanical properties; microstructure; residual stress

1 Introduction

Magnesium alloys are known as the lightest materials among different alloys applied around the world, and they are used widely in different industries namely the transportation and aero-space [1−3]. However, their poor ductility because of the hexagonal closed-pack (HCP) crystal structure causes a distinct restriction to using in different applications. Therefore, several studies have been carried out to improve the formability of magnesium alloy through texture and grain size modification [4−8]. Friction stir processing (FSP) is an example of severe plastic deformation (SPD) processes and it is an effective technique to refine the texture of the light-weight alloys such as aluminum and magnesium through dynamic recrystallization [9,10]. In FSP, a rotating tool, including a shoulder and a pin, is used. While the pin penetrates into the workpiece, the shoulder contacts the metal surface. Because of the contact between the tool and the workpiece, heat is produced, and the material of the sample surrounding the tool is softened. This material is locally stirred by the pin, and the microstructure within the stir zone is processed [11−15].

During FSP, the fine grain size in different ranges from nano-size to micro-size in the processed zone can be achieved. ABBASI et al [16]

Corresponding author: Behrouz BAGHERI; E-mail: b.bagheri@aut.ac.ir
DOI: 10.1016/S1003-6326(20)65264-5

analyzed the influences of two reinforcing particles, namely SiC and Al_2O_3 particles, on the mechanical, tribological and corrosion properties of surface composites developed on AZ91 magnesium alloy by FSP. It was indicated that specimens including SiC particles had higher strength, ductility, and also better corrosion resistance than those including Al_2O_3 particles. THAPLIYAL and DWIVEDI [17] studied the effect of FSP on microstructure and tribological behavior of the cast nickel aluminum bronze (C95500) alloy. They found that a fine equiaxed grain microstructure was developed in the stir zone by application of FSP and also by addition of the graphite particles, wear properties were improved by about 43% and 52% in comparison with both FS-processed specimen and as-cast surface, respectively. SAINI et al [18] analyzed the microstructure and wear behavior of Zn- and MoS_2-reinforced surface composite developed by FSP on Al−Si alloy. They reported that UTS (ultimate tensile strength) of MoS_2-reinforced Al−Si alloy was about 115 MPa and that of Zn-reinforced composite was about 85 MPa.

Recently, much has been done to improve the FSP technology [19−21]. MOUSAVIZADE et al [22] applied the laser to heat a localized region ahead of the FSP tool to provide sufficient plasticity during the FSP of the IN738LC superalloy. They found that laser-assisted friction stir processing (LAFSP) resulted in a defect-free stir zone and additionally, it led to ductility increase. They also found that LAFS-processed specimens had a coarser grain size in the stir zone compared with FS-processed specimens. KUMAR [23] designed a setup for applying vibration to the tool during FSP by ultrasonic waves. This method is entitled to ultrasonic-assisted friction stir processing (UaFSP). He studied the effects of UaFSP on microstructure and mechanical properties of processed specimens. He realized that ultrasonic vibration generated high heat in the stir zone and caused intense plastic deformation and improved the material flow. Higher ultimate tensile strength (UTS) and hardness were observed for the UaFS-processed specimens compared with the FS-processed specimens. BARADARANI et al [24] studied the effect of UaFSP on microstructure, corrosion behavior and mechanical properties of AZ91 magnesium alloy. The results revealed that the corrosion current density of UaFS-processed specimens was about 2.09 μA/cm^2, while it was about 3.42 μA/cm^2 for FS-processed specimens. They found that UaFSP altered the morphology and distribution of the β-$Mg_{17}Al_{12}$ phase and led to a better distribution of this phase compared to FSP.

There are significant drawbacks with respect to applying ultrasonic vibration to the tool during FSP, such as expensive equipment and additionally, it needs enough skill to work with the machine. To address these problems, a new modified version of FSP entitled “friction stir vibration processing (FSVP)” was introduced. In this method, the workpiece is vibrated mechanically through the camshaft mechanism. FSP and FSVP were applied to developing the surface composite on AZ91 magnesium alloy by incorporation of SiC particles.

2 Experimental

AZ91 magnesium alloy sheet with a thickness of 3 mm and the following chemical composition (wt.%): Al, 9.1; Zn, 0.68; Mn, 0.21; Si, 0.085; Fe, 0.0029; Cu, 0.0097; Ni, 0.001; Mg, the balance was used as the base metal matrix. The as-received microstructure of the base metal is presented in Fig. 1. The base metal alloy included α-phase and aluminum-rich β-phase ($Mg_{17}Al_{12}$) precipitates along the grain boundaries (Fig. 1).

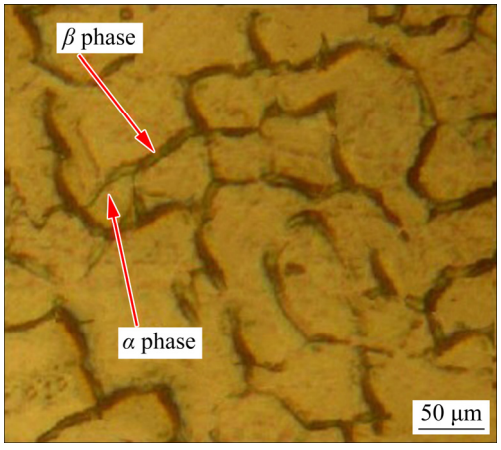

Fig. 1 Microstructure of as-received AZ91 magnesium alloy

Rectangular specimens with dimensions of 200 mm × 100 mm were prepared from the base metal sheet and V-shape grooves, with a depth of 1.5 mm and groove opening width of 2 mm, were cut on the surface of specimens along the length. SiC nanoparticles with different dimensions, 30 and

300 nm, were utilized as reinforcing particles. The particles were filled in the grooves. The same mass of particles, (0.06±0.002) g, was applied for each specimen. Before filling the grooves, the specimens were carefully deburred and cleaned to remove oil and debris by ethanol.

FSP and FSVP were carried out by a milling machine. For FSP, the specimens were fixed on a fixture and the fixture was installed on the milling machine. For FSVP, the specimens were fixed on the fixture and the fixture was installed on a machine designed and manufactured by the authors to vibrate the working specimens normal to tool transverse direction. A view of this machine is presented in Fig. 2. The machine works based on the camshaft mechanism. The rotating movement of a motor shaft is transformed into the linear and reciprocating movement of a vibrating plate through a camshaft. The vibration frequency is controlled by a driver and the vibration amplitude is 0.5 mm. In this work, vibration frequency, tool rotational speed, and tool transverse speed were 20 Hz, 1250 r/min, and 95 mm/min, respectively. The tilt angle of the tool was 2° and the tool had a clockwise rotation.

Two-pieces tool consisting of a shoulder and a pin was used for FSP and FSVP. The schematic design of the tool can be found in Ref. [25]. The shoulder and pin were prepared from M2 steel and carbide tungsten, respectively. To encapsulate the particles within the grooves, prior to FSP and FSVP, the surface of the specimens, in the groove position, was rubbed by a pin-less tool. This impeded the escape of particles from the groove during FSP and FSVP.

Metallography samples were prepared from the cross-sections of the processed specimens, and they were subjected to grinding, polishing, and etching. The test sections were mounted and manually ground with emery papers (80−2400 grit) and carefully polished using alumina powders with a size of 0.03 μm. The surfaces were etched by an etchant containing acetic acid (5 mL), nitric acid (7 mL), water (10 mL), picric acid (6 g), HCL (5 mL), and ethanol (100 mL) for 3−5 s. Scintag XDS2000 X-ray diffractometer was used to analyze X-ray diffraction (XRD). The scanning electron microscopy (SEM) and optical microscopy (OM) were used to observe the distribution of nano-sized SiC particles, material flow, and microstructure. In this study, JEM−2200FS TEM at 200 kV was applied to TEM analysis of processed samples.

Mechanical properties of the processed specimens were assessed using a uniaxial tensile test based on ASTM-E8 standard test [26]. Tensile test specimens were cut from the processed specimens employing wire electrical discharge machining (EDM) technology. The tensile test specimens were normal to the processing line and the stir zone was positioned in the middle and in the gauge section. Tensile tests were applied at room temperature by Instron tensile test machine with a strain rate of 1×10^{-5} s^{-1}. Three specimens were evaluated for each processing condition. The linear intercept method [27] was applied to measuring the grain size. To measure the grain size, a square of the selected area (400 μm × 400 μm) was overlaid on a micrograph and the numbers of grains including the grains completely within the area and one half of the number of grains intersected by the circumference of the area were counted. Assuming that the grains are circular, the number of grains per

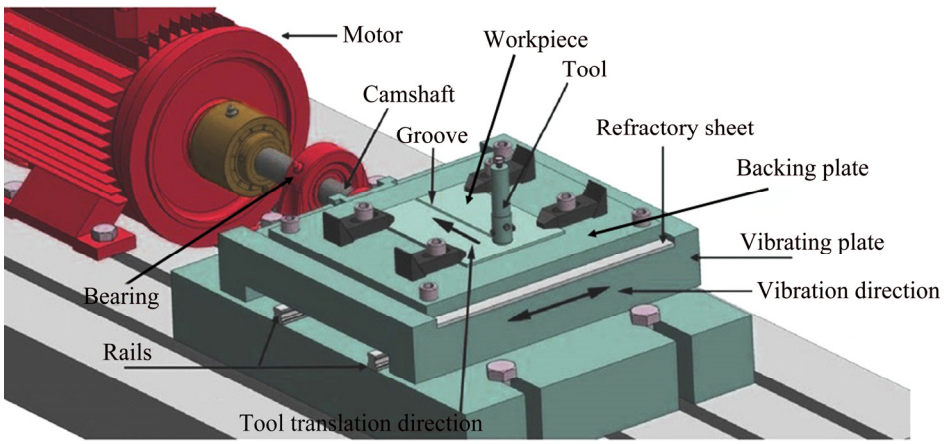

Fig. 2 Schematic view of machine used for FSVP

unit area was calculated and then, the average diameter of the grains was estimated. Vickers hardness (HV) technique was utilized to measure the microhardness of the processed specimens. Microhardness tests were performed on polished samples using a programmable hardness test machine. The load was 1 N and the dwell time was 10 s. For each processing condition, stir zone microhardness was measured three times and the mean value was reported.

3 Results and discussion

3.1 Microstructure

The microstructures showing particle distribution for FS- and FSV-processed specimens are presented in Fig. 3. It is observed that particle distribution of FSV-processed specimens is more homogenous than that of the FS-processed specimens and more agglomerates are observed for FS-processed specimens.

It is also observed in Fig. 3 that particle distribution homogeneity for small particles (30 nm) is better than that for large particles (300 nm). It is believed that material deformation during FSVP is higher than that during FSP. Workpiece vibration during FSVP, in addition to tool rotation and transverse motion, increases the material deformation in the stir zone. As a result, the particles are distributed more homogenously and less agglomerates occur during FSVP compared with FSP. Additionally, the motion of the material in the stir zone, during FSP and FSVP, transfers the small particles more easily than the large particles. So, small particles are distributed more homogenously than large particles.

Microstructures of stir zones for FS- and FSV-processed specimens are presented in Fig. 4. It is observed in Fig. 4 that grains for FSV-processed specimens are smaller than those for FS-processed specimens. This can be related to the role of vibration in FSVP. It has been known that dynamic recrystallization (DR) is the main reason for the grain refinement during FSP [28,29]. Material deformation in the stir zone generates dislocations and the density of dislocations increases as deformation increases [30]. High heat due to friction between tool and workpiece brings the possibility for the dislocations to move and arrange sub-grain boundaries and form low angle grain boundaries (LAGBs) with misorientation angels less than 15°. As deformation proceeds, misorientation angle increases and LAGBs change to high angle grain boundaries (HAGBs), and therefore grain refinement occurs [28]. In FSVP, due to the vibration effect of the workpiece, material deformation is higher than that in FSP. Correspondingly, more dislocations are produced, more intensified DR occurs and finer grain grains are developed.

3.2 Mechanical properties

Figure 5 shows the stress−strain curves of the base metal, FS- and FSV-processed samples under

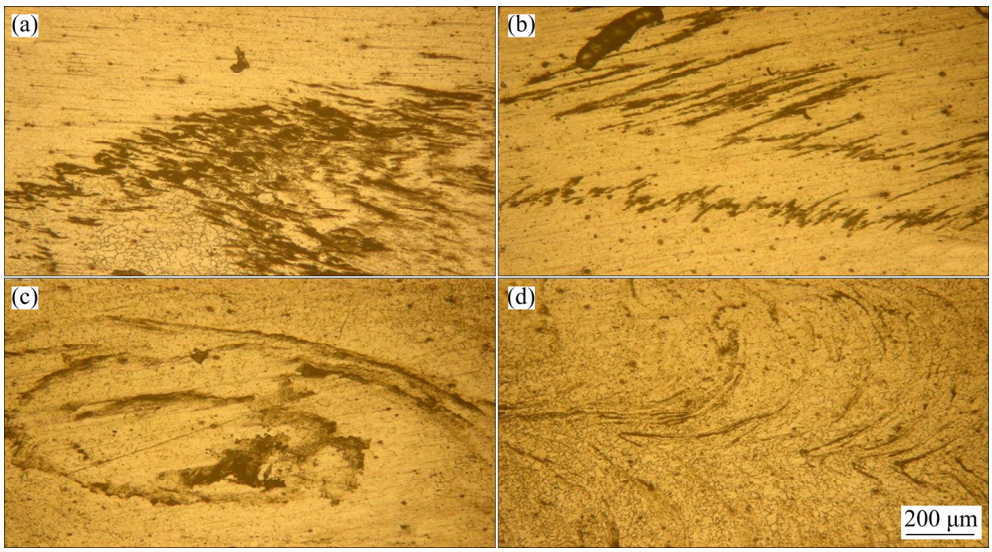

Fig. 3 Microstructures of different specimens showing particles distribution: (a) FSP with 300 nm SiC particles; (b) FSP with 30 nm SiC particles; (c) FSVP with 300 nm SiC particles; (d) FSVP with 30 nm SiC particles

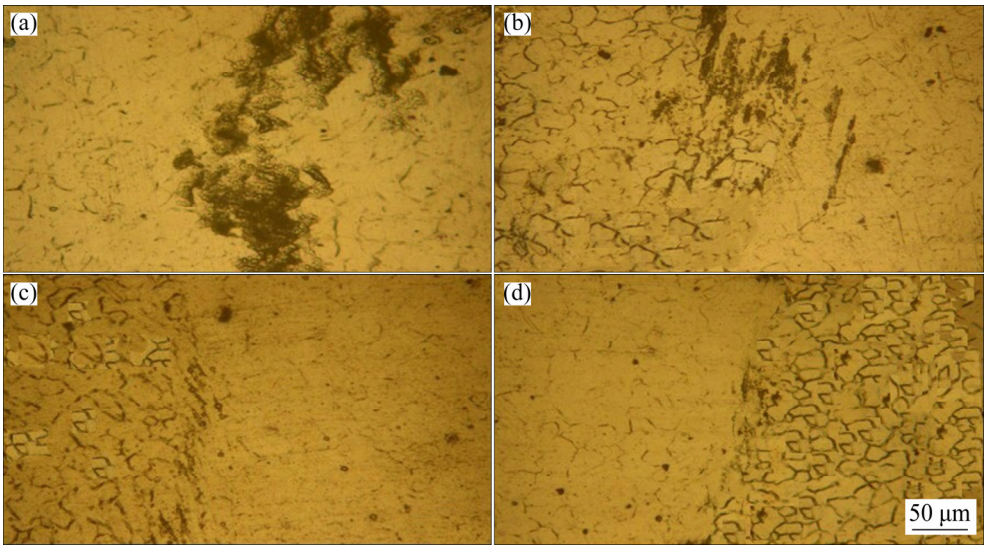

Fig. 4 Microstructures of stir zones in different samples: (a) FSP with 300 nm SiC particles; (b) FSP with 30 nm SiC particles; (c) FSVP with 300 nm SiC particles; (d) FSVP with 30 nm SiC particles

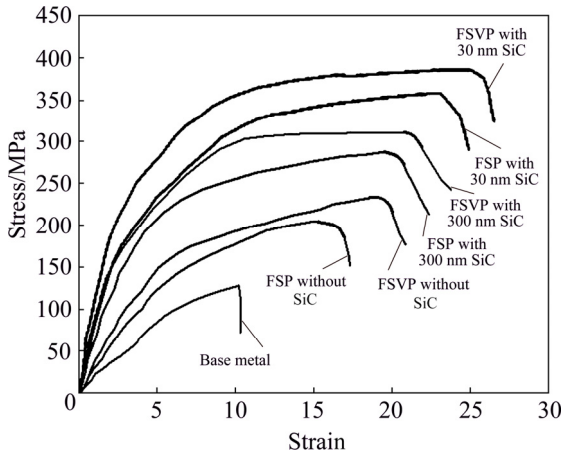

Fig. 5 Stress−strain curves of processed samples with different processing conditions and base metal

different processing conditions. Table 1 shows the elongation, tensile strength, and formability index of the specimens for both FSP and FSVP methods. It can be seen from data that the strength and ductility values of FS- and FSV-processed specimens are greater than those of the as-received specimen. The lower grain size of processed specimens, as well as the presence of second-phase particles, is the main reason for higher mechanical properties of processed specimens with respect to as-received specimens. As grain size decreases, the volume fraction of grain boundaries increases. Grain boundaries and second-phase particles inhibit the movement of dislocations and increase the strength [31].

The lower stir zone grain size and the more homogenous distribution of SiC particles might be the main reasons for better mechanical properties of FSV-processed specimens compared with FS-processed specimens. For a constant mass of SiC powders, a more homogenous distribution of SiC particles means less agglomeration of particles.

The strengthening by second-phase particles depends on the distribution of particles in the matrix. Volume fraction, shape, average particle diameter and mean interparticle spacing of particles are the main factors affecting the strengthening [31]. There are several ways in which the fine particles

Table 1 Mechanical properties of FS- and FSV-processed specimens under different conditions and base metal

Sample	UTS/ MPa	Elongation/ %	Formability index/ (MPa·%)
As-received	134.56	10.10	1359.0560
FSP without SiC particle	203.56	17.04	3465.2100
FSVP without SiC particle	231.14	19.83	4583.5062
FSP with 30 nm particle	323.14	23.94	7735.9716
FSP with 300 nm particle	273.23	20.46	5590.2858
FSVP with 30 nm particle	389.17	25.88	10071.7196
FSVP with 300 nm particle	311.85	22.04	6873.1740

Formability index is defined as product of UTS and elongation

can act as barriers to dislocations. The particles either may be cut by the dislocations or resist cutting and the dislocations are forced to bypass them [31]. A critical parameter of the dispersion of particles is the interparticle spacing (λ):

$$\lambda = \frac{4(1-f)r}{3f} \tag{1}$$

where f is the volume fraction of spherical particles with radius r. When the particles are small and/or soft, dislocations can cut and deform the particles. KELLY and NICHOLSON [32] found that the increment in strengthening ($\Delta\sigma$) is given by

$$\Delta\sigma = \frac{2\sqrt{6}}{\pi}\gamma_s \frac{f}{r} \tag{2}$$

where γ_s is the grain boundary tension (energy).

For the case of large particles, the degree of strengthening is determined by the shear stress required to bow a dislocation line between two particles separated by a distance λ. The stress required to force the dislocation between the obstacles (τ_0), according to Ref. [33] is

$$\tau_0 = \frac{\alpha G b}{\lambda}\ln\frac{r}{b} \tag{3}$$

where α is material constant, b is Burgers vector component, G is shear modulus. Based on Eq. (3) the effect of λ is greater than that of r. As homogeneity of particle distribution increases, agglomeration decreases. In this regard, for a constant value of volume fraction f, r and λ decrease and strengthening due to second-phase particles increases.

Interparticle spacing λ and size of particles r decrease as homogeneity of particle distribution enhances, and according to Eqs. (2) and (3) strength increases as r and λ decrease. It should be mentioned that large agglomerated particles are enumerated as stress concentration sites and cracks can be initiated from them.

Grain boundaries not only impede the movement of dislocations but also decrease the crack growth and increase the ductility. ESTRIN et al [34] found that the fracture mechanism changed from intergranular fracture to transgranular fracture as grain size decreased. LI and CUI [35] found that the volume fraction of GNDs (geometrically necessary dislocations) increased as grain size decreased. GNDs accommodate the strain between different grains in the microstructure and they can postpone the crack initiation. In this regard, higher ductility is anticipated for the FSV-processed specimens compared with the FS-processed specimens. The formability index which is representative of toughness is the ability of a substance to deform without fracture [36]. Based on Table 1, the formability index values of FSV-processed specimens are higher than those of FS-processed specimens. It is related to higher UTS and ductility values of the former specimen with respect to the latter specimen.

According to the results in Table 1, the strength and ductility values of processed specimens containing small SiC particles are higher than those relating to specimens containing large particles. This can also be related to a more homogenous distribution of strengthening particles in the former specimens, which leads to higher strength and ductility. A more homogenous distribution of strengthening particles is observed in Fig. 3 for small size particles compared with large size particles.

Figure 6 presents the microhardness profiles of different specimens under FSP and FSVP conditions. The highest hardness values are observed for FSV-processed specimens containing small SiC particles. Hardness values of FSV-processed specimens are larger than those for FS-processed specimens and hardness values of processed specimens containing small particles are larger than those containing large particles.

Hardness is a measure of the material resistance to localized plastic deformation [37]. So, hardness increases as the dislocation movement

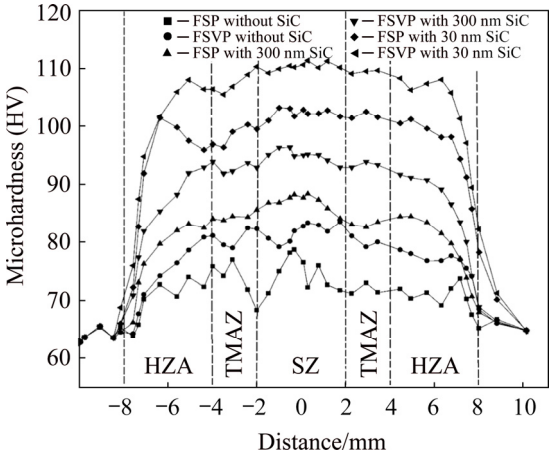

Fig. 6 Influence of vibration and reinforcing particle size on microhardness values of stir zone for FS- and FSV-processed specimens

decreases. It was noted before that grain boundaries and second-phase particles decreased the movement of dislocations [31]. It was observed in Fig. 4 that volume fraction of grain boundaries for FSV-processed specimens, due to finer grains, is higher than that for FS-processed specimens. So, higher hardness values of FSV-processed compared to FS-processed specimens are reasonable. Correspondingly, higher hardness values are anticipated for processed specimens containing SiC particles with respect to specimens without strengthening particles because SiC particles inhibit the movement of dislocations. It was noted before that more homogenous distribution of strengthening particles and less agglomeration of these particles (lower λ and r values) led to higher strength. It is observed in Fig. 6 that hardness values of specimens containing small SiC particles are higher than those of specimens containing large SiC particles.

3.3 Fracture morphology

The fracture surface images of processed specimens by FSP and FSVP methods are shown in Fig. 7. The presence of dimples indicates that all specimens show a ductile fracture. Ductile fracture is usually preceded by a localized reduction in diameter called necking [38]. Fine cavities form in the necked region and under continued straining, the cavities grow and coalesce into a crack. While the crack grows in the direction transverse to the tensile axis, on a finer scale the crack has zig-zags back and forth across the transverse plane by void-sheet formation. Thus, crack growth in the ductile fracture is essential by a process of void coalescence [38]. Coalescence occurs by elongation of the voids and elongation of the bridges of material between the voids. This leads to the formation of a fracture surface consisting of elongated dimples as it is formed from numerous holes which are separated by thin walls until it fractures. Inclusions, second-phase particles or fine oxide particles are the primary sites for void formation, while in high-purity metals voids can form at grain boundary triple points and dislocation locks [39,40]. It has been found that voids on primary sites are larger than those at grain boundaries and dislocation locks [41].

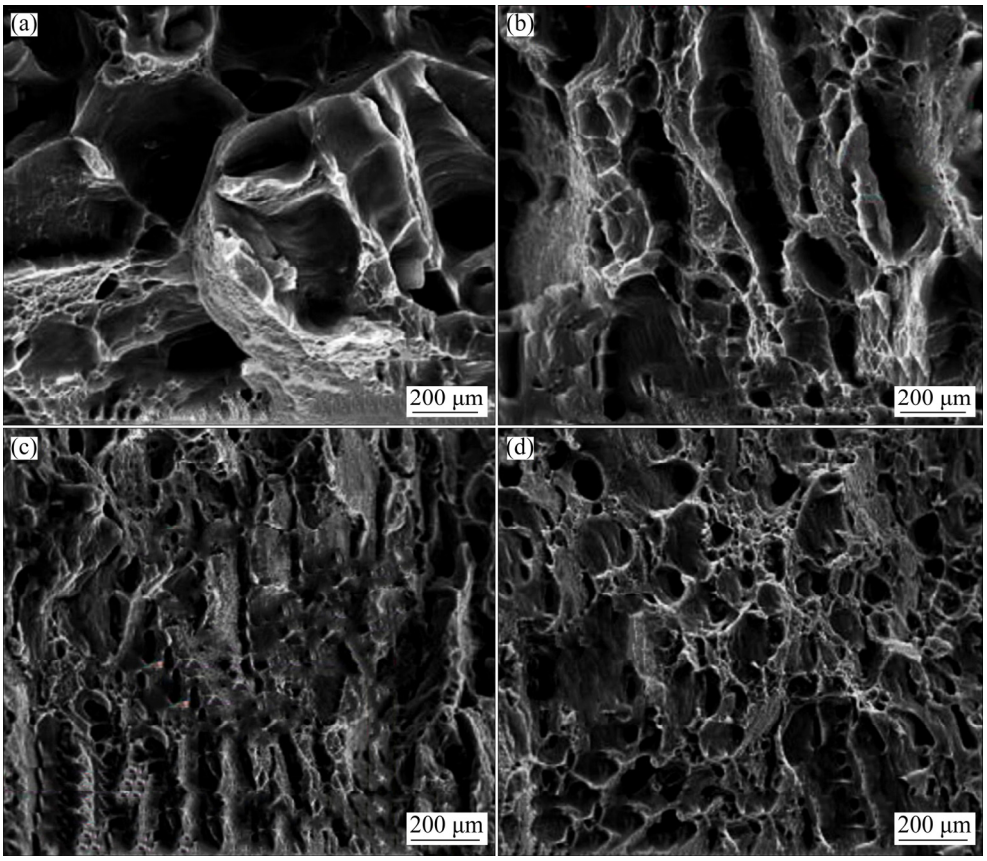

Fig. 7 Fracture surfaces images of different specimens: (a) FSP with large SiC particle size; (b) FSP with small SiC particle size; (c) FSVP with large SiC particle size; (d) FSVP with small SiC particle size

It is observed that dimples for processed specimens containing large particles are larger than those for processed specimens containing small particles, and voids for FS-processed specimens are larger than those for FSV-processed specimens. These can be related to the distribution of particles. It was noted before that particle distribution for small particles was more homogenous than that for large particles and less agglomeration occurred for small particles. Additionally, it was mentioned before that particle distribution for FSV-processed specimens was more homogenous than that for FS-processed specimen. Large agglomerated particles were primary sites for the constitution of large voids [41]. So, the presence of larger voids on the fracture surface of processed specimens containing large particles compared to specimens containing small particles and on the fracture surface of FSV-processed specimens compared to FS-processed specimens is reasonable.

3.4 Effect of vibration frequency

In this section, the microstructure and mechanical characteristics of FSV-processed specimens containing SiC particles with a size of 30 nm and processed with different vibration frequencies namely 25, 35 and 50 Hz were studied. OM images of stir zone of processed specimens with different vibration frequencies are presented in Fig. 8. It is found that stir zone grain size decreases as vibration frequency increases. This can be related to the effect of vibration during FSVP. As vibration frequency increases, material deformation in the stir zone increases [42]. It has been found that there is a direct relationship between the dislocation density and the material deformation, and the dislocation density increases as the material deformation increases [30]. As the density of dislocations increases, the occurrence of dynamic recrystallization is intensified [42]. The greater the dynamic recrystallization is, the better the grain refinement is.

TEM analysis was carried out to investigate the influence of vibration frequency on nano-sized SiC particle distribution in the AZ91 composite layer. TEM images of processed specimens with different vibration frequencies are delivered in Fig. 9. Figure 9 shows how particles distribute in the microstructure for different vibration frequencies. It is observed in Fig. 9 that particle

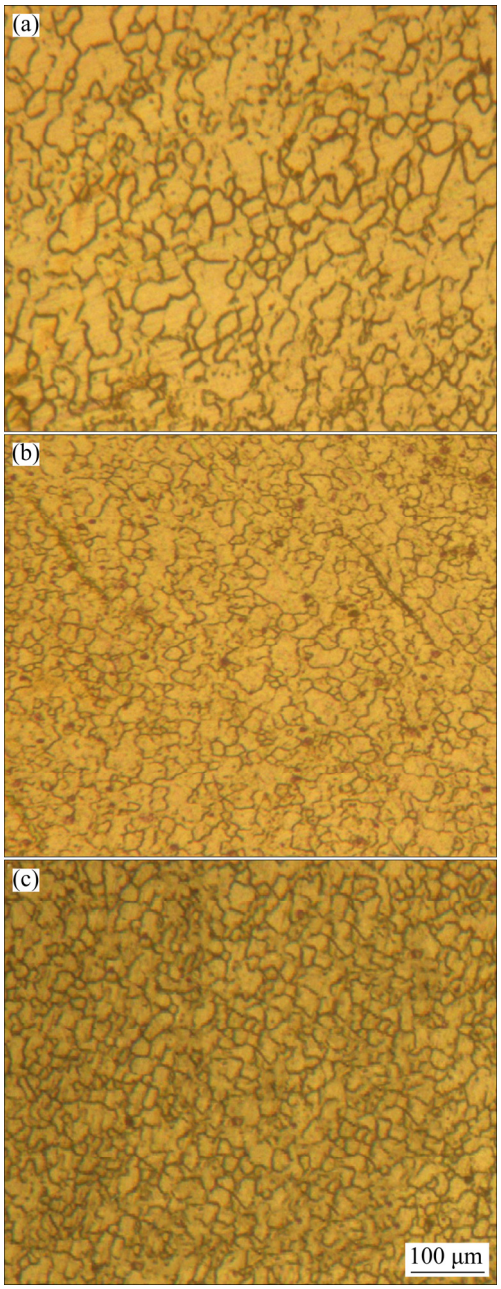

Fig. 8 OM images of stir zone for FSV-processed samples at different frequencies: (a) 25 Hz; (b) 35 Hz; (c) 50 Hz

distribution for the processed specimen with a vibration frequency of 50 Hz is more homogenous than other specimens. Figure 9 also indicates that the homogeneity of particle distribution increases as vibration frequency increases. As vibration frequency increases, the material in the stir zone is stirred and deformed more seriously and as a result, less agglomeration of particles occurs and the particles are distributed more homogeneously.

Figure 10 presents the XRD patterns of the processed specimens under different vibration

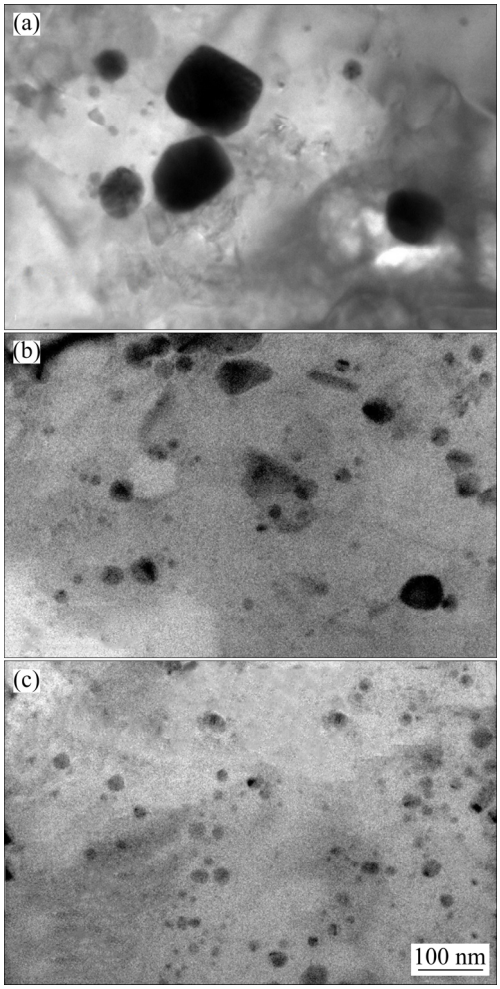

Fig. 9 TEM images of SiC particle distribution and agglomeration during FSVP at different vibration frequencies: (a) 25 Hz; (b) 35 Hz; (c) 50 Hz

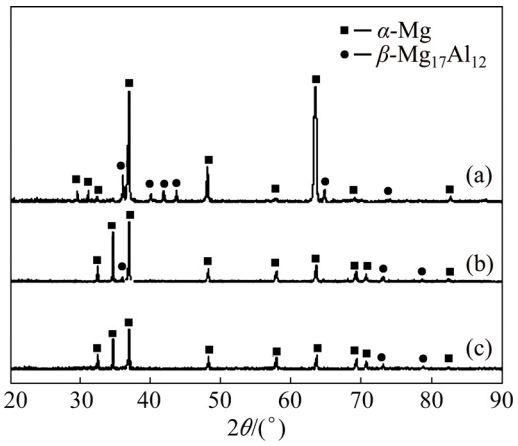

Fig. 10 XRD patterns of FSP-processed specimens with 300 nm SiC particles under different vibration frequencies: (a) 25 Hz; (b) 35 Hz; (c) 50 Hz

frequencies. It is clear that the number and the intensity of β-phase ($Mg_{17}Al_{12}$) peaks decrease as vibration frequency increases. The main reason is the dissolution of β-phase in the α-Mg matrix during FSVP. It has been found that β-phase is dissolved during FSP because of high temperature [23]. BAROONI et al [43] found that peak temperature in the stir zone during FSVP, due to higher deformation of the material, is higher than that during FSP and peak temperature in FSVP increases as vibration frequency increases. So, more dissolution of β-phase is anticipated for FSVP compared with FSP and higher dissolution of β-phase occurs as vibration frequency increases during FSVP.

Figure 11 shows the mechanical properties of processed specimens with different vibration frequencies during FSVP. It can be distinguished that the strength and ductility, as well as hardness, are improved as frequency increases.

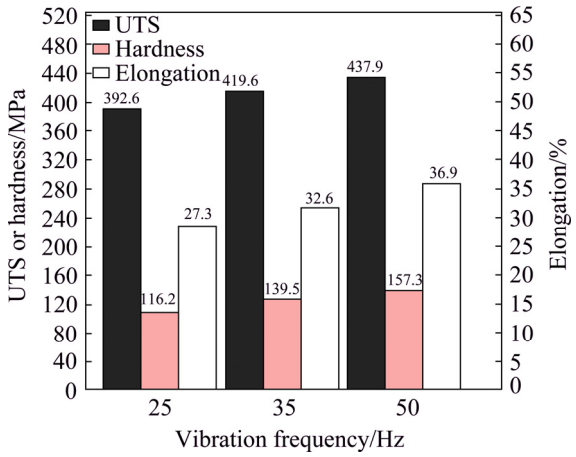

Fig. 11 Mechanical properties of FSV-processed samples at different vibration frequencies

These can be related to the effect of grain size and particle distribution. It is observed that stir zone grain size decreases (Fig. 8) and particles distribute more homogenously as vibration frequency increases (Fig. 9). As grain size decreases, the volume fraction of grain boundaries increases and the movement of dislocations decreases [31]. According to Hall−Petch relation: $\sigma=\sigma_0+kd^{-1/2}$, strength σ increases as grain size d decreases. As a result, finer grains lead to higher strength and hardness. The presence of SiC particles also decreases the movement of dislocations and enhances strength and hardness. According to Eqs. (2) and (3), the more homogenous distribution of second-phase particles (lower λ and r values) results in higher strength and hardness. Figure 11

also reveals that ductility increases as vibration frequency increases. The higher volume fraction of grain boundaries, as well as GNDs and more homogenous distribution of strengthening particles are some reasons for ductility improvement as vibration frequency increases.

Figure 12 shows the longitudinal residual stress profiles for FSV-processed specimens at different vibration frequencies. It is evident that the longitudinal residual stress increases as vibration frequency increases. The maximum value is about 88 MPa for the processed specimens under a vibration frequency of 50 Hz, while this value is around 72 MPa for specimens processed under the vibration frequency of 25 Hz. Residual stresses are developed in solid materials due to non-uniform distribution of deformation or temperature during a process such as welding, heat treatment or deformation [44]. As vibration frequency during FSVP increases, the material deformation in the stir zone increases and as a result, the difference between the stir zone and the surrounding material, regarding the deformation, increases. This leads to the development of higher residual stress as vibration frequency increases.

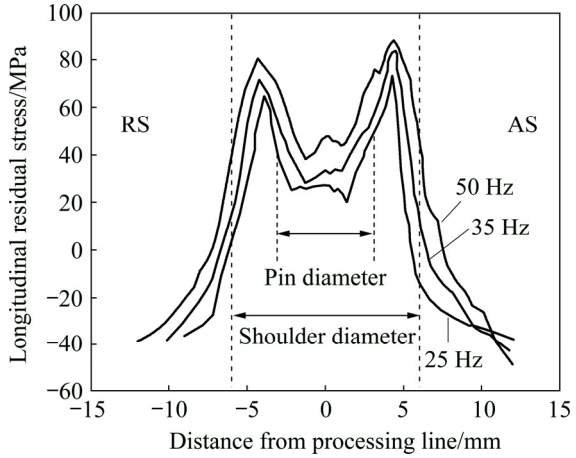

Fig. 12 Longitudinal residual stress profiles of FSV-processed specimens at different vibration frequencies

4 Conclusions

(1) A modified version of FSP with the title of "friction stir vibration processing (FSVP)" was applied to developing surface composites on the AZ91 magnesium alloy. Nano-sized SiC particles with different sizes, 30 and 300 nm, were incorporated as strengthening particles. The effects of workpiece vibration and size of strengthening particles on the microstructure and mechanical properties of AZ91 composite layers were studied. The results indicated that stir zone grain size decreased and also reinforcing particles distributed more uniformly as the vibration was applied in FSVP.

(2) Hardness, strength, and ductility of FSV-processed specimens, due to more intensified dynamic recrystallization, were higher than those of FS-processed specimen. The tensile strength value for the FS-processed specimen was around 204 MPa, while it was about 232 MPa for the FSV-processed specimen without SiC strengthing particles.

(3) The effect of small SiC particles (30 nm) on mechanical properties is greater than that for large SiC particles (300 nm). The results showed that small strengthening particles distributed more homogenously than large particles during FSP and FSVP. The ductility and formability index values increased respectively from about 22% and 6873 MPa·% for FSV-processed specimen containing large SiC particles (300 nm) to about 26% and 10072 MPa·% for FSV-processed specimen containing small particles (30 nm), respectively.

(4) The role of FSVP on microstructure and mechanical properties increased as vibration frequency increased. Hardness value in the stir zone increased from about 116 MPa for FSV-processed specimen at vibration frequency of 25 Hz to about 157 MPa for FSV-processed specimen at vibration frequency of 50 Hz.

(5) Higher tensile residual stresses developed in the stir zone of FSV-processed specimens as vibration frequency increased.

Acknowledgments

The authors would like to thank the Amirkabir University of Technology (AUT), Sharif University of Technology and National Elites Foundation of Iran for their support during this research.

References

[1] BAGHERI B, ABBASI M. Development of AZ91/SiC surface composite by FSP: Effect of vibration and process parameters on microstructure and mechanical characteristics [J]. Advances in Manufacturing Journal, 2020, 8: 82−86.

[2] ABBASI M, ABDOLLAHZADEH A, BAGHERI B, OMIDVAR H. The effect of SiC particle addition during

FSW on microstructure and mechanical properties of AZ31 magnesium alloy [J]. International Journal Materials Engineering and Performance, 2015, 24: 5037−5045.

[3] ROSE A R, MANISEKAR K, BALASUBRAMANIAN V. Influences of welding speed on tensile properties of friction stir welded AZ61A magnesium alloy [J]. Journal of Materials Engineering and Performance, 2012, 21: 257−265.

[4] ABBASI M, ABDOLLAHZADEH A, OMIDVAR H, BAGHERI B, REZAEI M. Incorporation of SiC particles in FS welded zone of AZ31 Mg alloy to improve the mechanical properties and corrosion resistance [J]. International Journal of Materials Research, 2016, 107: 566−572.

[5] ABDOLLAHZADEH A, SHOKUHFAR A, OMIDVAR H, CABRERA J M, SOLONIN A, OSTOVARI A, ABBASI M. Structural evaluation and mechanical properties of AZ31/SiC nano-composite produced by friction stir welding process at various welding speeds [J]. Journal of Materials: Design and Applications, 2019, 233: 831−841.

[6] DEEPAN M, PANDEY C, SAINI N, MAHAPATRA M M, MULIK R S. Estimation of strength and wear properties of Mg/SiC nanocomposite fabricated through FSP route [J]. Journal of the Brazilian Society of Mechanical Sciences and Engineering, 2017, 39: 4613−4622.

[7] ABDOLLAHZADEH A, SHOKUHFAR A, CABRERA J M, ZHILYAEV A P, OMIDVAR H. In-situ nanocomposite in friction stir welding of 6061-T6 aluminum alloy to AZ31 magnesium alloy [J]. Journal of Materials Processing Technology, 2019, 263: 296−307.

[8] KEIVANI R, BAGHERI B, SHARIFI F, KETABCHI M, ABBASI M. Effects of pin angle and preheating on temperature distribution during friction stir welding operation [J]. Transactions of Nonferrous Metals Society of China, 2013, 23: 2708−2713.

[9] ABDOLLAHZADEH A, SHOKUHFAR A, CABRERA J M, ZHILYAEV A P, OMIDVAR H. The effect of changing chemical composition on dissimilar Mg/Al friction stir welded butt joints using zinc interlayer [J]. Journal of Manufacturing Processes, 2018, 34: 18−30.

[10] FALLAHI A A, SHOKUHFAR A, MOGHADDAM A O, ABDOLAHZADEH A. Analysis of SiC nano-powder effects on friction stir welding of dissimilar Al−Mg alloy to A316L stainless steel [J]. Journal of Manufacturing Processes, 2017, 30: 418−430.

[11] DADAEI M, OMIDVAR H, BAGHERI B, JAHAZI M, ABBASI M. The effect of SiC/Al_2O_3 particles used during FSP on mechanical properties of AZ91 magnesium alloy [J]. International Journal of Materials Research, 2014, 105: 369−374.

[12] ABBASI M, GIVI M, BAGHERI B. Application of vibration to enhance efficiency of friction stir processing [J]. Transactions of Nonferrous Metals Society of China, 2019, 29: 1393−1400.

[13] ZHANG D T, XIONG F, ZHANG W W, CHENG Q, ZHANG W. Superplasticity of AZ31 magnesium alloy prepared by friction stir processing [J]. Transactions of Nonferrous Metals Society of China, 2011, 21: 1911−1916.

[14] SURYA KIRAN G V V, HARI KRISHNA K, SAMEER S K, BHARGAVI M, SANTOSH KUMAR B, MOHANA RAO G, NAIDUBABU Y, DUMPALA R, RATNA SUNIL B. Machining characteristics of fine grained AZ91 Mg alloy processed by friction stir processing [J]. Transactions of Nonferrous Metals Society of China, 2017, 27: 804−811.

[15] AKYUZ B. Influence of Al content on machinability of AZ series Mg alloys [J]. Transactions of Nonferrous Metals Society of China, 2013, 23: 2243−2249.

[16] ABBASI M, BAGHERI B, DADAEI M, OMIDVAR H R, REZAEI M. The effect of FSP on mechanical, tribological, and corrosion behavior of composite layer developed on magnesium AZ91 alloy surface [J]. The International Journal of Advanced Manufacturing Technology, 2015, 77: 2051−2058.

[17] THAPLIYAL S, DWIVEDI D K. Microstructure evolution and tribological behavior of the solid lubricant based surface composite of cast nickel aluminum brone developed by friction stir processing [J]. Journal of Materials Processing Technology, 2016, 238: 30−38.

[18] SAINI N, PANDY C, THAPLIYAL S, DWIVEDI D K. Mechanical properties and wear behavior of Zn and MoS_2 reinforced surface composite Al−Si alloys using friction stir processing [J]. Silicon, 2018, 10: 1979−1990.

[19] FOULADI S, ABBASI M. The effect of friction stir vibration welding process on characteristics of SiO_2 incorporated joint [J]. Journal of Materials Processing Technology, 2017, 243: 23−30.

[20] BAGHERI B, ABBASI M, ABDOLLAHZADEH A, OMIDVAR H. Advanced approach to modify friction stir spot welding process [J]. Metals and Materials International, 2020: 1−12. (Article in press)

[21] BAGHERI B, ABBASI M, ABDOLLAHZADEH A, KOKABI A H. A comparative study between friction stir processing and friction stir vibration processing to develop magnesium surface nanocomposite [J]. International Journal of Minerals, Metallurgy and Materials, 2020: 1−22. (Article in press)

[22] MOUSAVIZADE S M, POURANVARI M, GHAINI F M, FUJII H, CHUNG Y D. Laser-assisted friction stir processing of IN738LC nickel-based superalloy: Stir zone characteristics [J]. Science and Technology of Welding and Joining, 2016, 21: 374−380.

[23] KUMAR S K. Ultrasonic assisted friction stir processing of 6063 aluminum alloy [J]. Archives of Civil and Mechanical Engineering, 2016, 16: 473−484.

[24] BARADARANI F, MOSTAFAPOUR A, SHALVANDI M. Enhanced corrosion behavior and mechanical properties of AZ91 magnesium alloy developed by ultrasonic-assisted friction stir processing [J]. Materials and Corrosion, 2020, 71: 109−117.

[25] BARATI M, ABBASI M, ABEDINI M. The effects of friction stir processing and friction stir vibration processing on mechanical, wear and corrosion characteristics of $Al6061/SiO_2$ surface composite [J]. Journal of Manufacturing Processes, 2019, 45: 491−497.

[26] ASTM−E8M. Standard test methods for tension testing of metallic material [S]. West Conshohocken, PA: ASTM International, USA, 2016.

[27] ASTM−E112−13. Standard test methods for determining

average grain size [S]. West Conshohocken, PA: ASTM International, USA, 2013.
[28] SU J Q, NELSON T W, STERLING C J. Grain refinement of aluminum alloys by friction stir processing [J]. Philosophical Magazine, 2006, 86: 1−24.
[29] ABDOLAHZADEH A, OMIDVAR H, SAFARKHANIAN, M A, BAHRAMI M. Studying microstructure and mechanical properties of SiC-incorporated AZ31 joints fabricated through FSW: The effects of rotational and traveling speeds [J]. The International Journal of Advanced Manufacturing Technology, 2014, 75: 1189−1196.
[30] HULL D, BACON D J. Introduction to dislocations [M]. 5th ed. Amsterdm: Elseviter, 2011.
[31] DITER G E, BACON D. Mechanical and metallurgy [M]. London: McGraw-Hill, 1988.
[32] KELLY A, NICHOLSON R B. Precipitation hardening [J]. Progress in Materials Science, 1963, 10: 151−158.
[33] ASHBY M F. The mechanical effects of a dispersion of a second phase [C]//Proceedings of the Second International Conference on the Strength of Metals II, ASM. Pacific Grove, California, 1970: 507−541.
[34] ESTRIN Y Z, ZABRODIN P A, BRAUDE I S, GRIGOROVA T V, IASEV N V, PUSTOVALOV V V, FOMENKO V S, SHUMILIN S E. Low temperature plastic deformation of AZ31 magnesium alloy with different microstructures [J]. Low Temperature Physics, 2010, 36: 1100−1112.
[35] LI S X, CUI G R. Dependence of strength, elongation and toughness on grain size in metallic structural materials [J]. Applied Physics, 2007, 101: 1−6.
[36] NADERI M , ABBASI M, SAEED-AKBARI A. Enhanced mechanical properties of a hot-stamped advanced high-strength steel via tempering treatment [J]. Metallurgy and Materials Transaction A, 2013, 44: 1852−1861.
[37] BAGHERI B, ABBASI M, GIVI M. Effects of vibration on microstructure and thermal properties of friction stir spot welded (FSSW) aluminum alloy (Al5083) [J]. International Journal of Precision Engineering and Manufacturing, 2019, 20(7): 1219−1227.
[38] HERTZBERG R W. Deformation and fracture mechanics of engineering materials [M]. 4th ed. New York: John Wiley & Sons, USA, 1996.
[39] PANDEY C, SAINI N, MAHAPATRA M M, KUMAR P. Study of the fracture surface morphology of impact and tensile tested cast and forged (C&F) grade 91 steel at room temperature for different heat treatment regimes [J]. Engineering Failure Analysis, 2017, 71: 131−147.
[40] PANDEY C, SAINI N, MAHAPATRA M M, KUMAR P. Hydrogen induced cold cracking of creep resistant ferritic P91 steel for different diffusible hydrogen levels in deposited metal [J]. International Journal of Hydrogen Energy, 2016, 41: 17695−17712.
[41] UTHAISANGSUK V. Microstructure based formability modeling of multiphase steels [D]. Aachen: RWTH Achen University, 2009.
[42] BAGHERI B, ABBASI M, DADAEI M. Mechanical behavior and microstructure of AA6061-T6 joints made by friction stir vibration welding [J]. Journal of Material Engineering and Performance, 2020, 29: 1165−1175.
[43] BAROONI O, ABBASI M, GIVI M, BAGHERI B. New method to improve the microstructure and mechanical properties of joint obtained using FSW [J]. International Journal of Advanced Manufacturing Technology, 2017, 93: 4371−4378.
[44] CALLISTER W D. Materials science and engineering: An introduction [M]. New York: John Wiley & Sons, 2003.

第二相粒径和振动对 FSP 制备 AZ91/SiC 表面复合层的影响

Behrouz BAGHERI[1], Mahmoud ABBASI[2], Amin ABDOLLAHZADEH[3,4], Seyyed Ehsan MIRSALEHI[1]

1. Department of Mining and Metallurgy, Amirkabir University of Technology, Tehran, Iran;
2. Faculty of Engineering, University of Kashan, Kashan, Iran;
3. Department of Materials Science and Engineering, Sharif University of Technology, Tehran, Iran;
4. Institute of Materials Engineering and Advanced Processes, Department of Mining and Metallurgy, Amirkabir University of Technology, Tehran, Iran

摘　要：采用改进的搅拌摩擦加工方法 (FSP) 加工 AZ91 镁合金试样。这种新方法称为“振动搅拌摩擦加工方法 (FSVP)”。SiC 纳米颗粒作为第二相粒子，利用 FSP 和 FSVP 制备合金的表面复合层，研究不同粒径(30 nm 和 300 nm) 的 SiC 强化颗粒对复合材料表面不同性能的影响。结果表明，采用 FSVP 工艺能细化材料的显微组织，提高材料的硬度、延展性和强度等力学性能。粒径为 30 nm 的增强颗粒对复合材料显微组织和力学性能的影响大于粒径为 300 nm 的增强颗粒。振动频率越高，FSV 试样的力学性能和显微组织越好；当 FSV 振动频率为 50 和 25 Hz 时，搅拌区硬度值分别约为 157 和 116 MPa。

关键词：搅拌摩擦加工；振动；SiC 纳米颗粒；粒径；力学性能；显微组织；残余应力

(Edited by Wei-ping CHEN)